

UNCLASSIFIED

AD NUMBER
ADB189727
NEW LIMITATION CHANGE
TO Approved for public release, distribution unlimited
FROM Distribution authorized to U.S. Gov't. agencies and their contractors; Administrative/Operational Use; 05 APR 1962. Other requests shall be referred to National Aeronautics and Space Administration, Washington, DC 20546.
AUTHORITY
NASA TR Server Website

THIS PAGE IS UNCLASSIFIED

APR 1962

0071 0

AD-B189 727



107,638

SOME APPLICATIONS OF DETAILED WIND PROFILE DATA
TO LAUNCH VEHICLE RESPONSE PROBLEMS

By Homer G. Morgan and Dennis F. Collins, Jr.

NASA Langley Research Center
Langley Air Force Base, Va.

For Presentation at the
Launch Vehicles: Structures and Materials Conference

Accession For	
NTIS CRA&I	<input type="checkbox"/>
DTIC TAB	<input checked="" type="checkbox"/>
Unannounced	<input type="checkbox"/>
Justification	
By _____	
Distribution/	
Availability Codes	
Dist	Avail and or Special

Phoenix, Arizona
April 3-5, 1962

DTIC
ELECTE
SEP 01 1994
S G D



94-26592



AD-107,638
94 8 19 1 2

SOME APPLICATIONS OF DETAILED WIND PROFILE DATA
TO LAUNCH VEHICLE RESPONSE PROBLEMS

By Homer G. Morgan* and Dennis F. Collins, Jr.*

NASA Langley Research Center

SUMMARY

The response of a launch vehicle to a number of detailed wind profiles has been determined. The wind profiles were measured by two techniques which are briefly described. One of these techniques uses an angle-of-attack sensor in conjunction with guidance data to measure the wind profile traversed by some particular launch vehicle. The other wind-measuring technique is a photographic triangulation method, whereby two cameras take simultaneous pictures of a vertical trail of smoke left by a launch vehicle or sounding rocket. The response of a vehicle flying these detailed profiles is compared with the response of the same vehicle flying through balloon-measured profiles. The response to the detailed wind profiles, relative to the balloon-measured profiles, is characterized by the large excitation of the rigid pitch and elastic bending modes. This is found to cause higher loads on the launch vehicle structure. Established design criteria which utilize balloon-measured wind profiles have arbitrarily accounted for this increased load by adding a load due to some type of discrete gust.

INTRODUCTION

The wind and gust criteria for determining design loads on launch vehicles, and the analytical methods by which these criteria are applied, reflect the characteristics of available wind and gust data. The wind data have been obtained primarily from balloon soundings which detect only the gross motion of the atmosphere and filter out the small-scale fluctuations as indicated in figure 1. Examples of design criteria based on such wind data are the synthetic wind profiles of references 1 through 4 and the measured profiles in references 3 and 5. Most of the gust data which have been available were for vertical gusts (or turbulence) measured by a horizontally flying airplane, references 6, 7, and 8, also indicated in the figure. The gust velocities have been assumed isotropic and criteria based on vertical gust data for application to horizontally flying vehicles (airplanes) have been adapted to vertically flying vehicles. Vehicle loads are usually predicted utilizing a rigid-body variable coefficient analysis with the wind profile as a forcing function

*Aerospace Technologist.

and an elastic-body fixed coefficient analysis with the gust as a forcing function. Total design loads are then found by combining loads from the two sources - winds and gusts. The shortcomings of these criteria and analytical techniques are well known, but improvements have awaited the availability of better wind and gust data.

Recently, wind and gust data of an improved nature have begun to become available. These data have been obtained by techniques which do not filter out the small-scale fluctuations of the wind and allow the wind and horizontal gust profile to be obtained simultaneously, references 9, 10, and 11. While these data are too new and too meager for design criteria utilizing them to have been established, the analytical techniques for predicting wind and gust loads must be reconsidered in view of the improved data.

In this paper a brief discussion of two of the methods for obtaining detailed wind profile data will be given. Wind data obtained by these methods will then be used to predict the loads and responses of a solid-propellant launch vehicle. The loads are determined using a program which accounts for the elasticity of the booster as well as the varying coefficients of the different equations. Comparisons are made with the loads which would have been predicted if the wind had been measured by a sounding balloon.

SYMBOLS

M	bending moment, lb-in.
M_{detailed}	bending moment induced by a detailed wind profile, lb-in.
M_{limit}	limit bending moment, lb-in.
M_{smoothed}	bending moment induced by a balloon-type wind profile, lb-in.
V_a	relative airstream velocity, ft/sec
V_i	inertial velocity, ft/sec
V_w	wind velocity, ft/sec
y	translation normal to a reference trajectory, in.
α	angle of attack, radians
γ	flight-path angle, radians
θ	attitude angle, radians

DETAILED WIND PROFILE DATA

Gusts and winds for application to vertically rising launch vehicles are differentiated only by their wavelengths. This distinction has been made primarily because of the form of available data. If data were available which described the motion of the atmosphere with enough detail, so that both the long and short wavelength variations were included, the wind and gust design criteria could be combined. Such data are also needed for the analysis of particular missile flights, either for evaluation of design criteria, for comparison of measured and calculated loads, or for failure investigations. In recent years, such data have begun to be collected by a number of methods. Two such techniques will be briefly described and examples of the data presented.

Angle-of-Attack Vane Method

The α -vane method, described in considerable detail in reference 9, makes use of sensor equipment carried routinely on many launch vehicles for guidance and control functions. A sketch of the measuring scheme is shown in figure 2, following reference 9, for the pitch plane only. Similar measurements in the yaw plane will determine the other component of wind. An initial assumption is made that the wind velocity V_w is horizontal. (As illustrated here, the wind is a headwind.) The vehicle's inertial velocity V_i , its flight-path angle γ , and its attitude angle θ are the quantities measured normally for guidance and control. An angle-of-attack sensor measures the angle α , between the vehicle axis and the free-stream velocity. This sensor is carried as part of the guidance and control equipment on some vehicles, or it may be added for this specific purpose. These measurements provide enough information to determine the wind velocity in whatever time or altitude increments are required, provided the data are continuous. Since winds measured by this technique are exactly those experienced by the flight vehicle, these data are especially useful for loads analysis of the particular flight.

An example of data obtained by this method is presented in figure 3. These data, similar to those of reference 9, were obtained from Mr. W. W. Vaughan of Marshall Space Flight Center. For comparison, the wind profile as measured by a radiosonde balloon released about 30 minutes after the vehicle launch is also given. Only the lower altitude portions of the east-west components are presented, since these produce the principal loadings on a vehicle. This figure shows the short wavelength variations in the α -vane wind profile which do not appear in the radiosonde balloon-measured profile (for example, at 25,000 feet altitude). It should be noted that the primary function of the instrumentation used to obtain this α -vane wind data was guidance and control

and the wind data were obtained only as a byproduct. The α -vane data have been reduced to give a wind velocity in 1/2-second intervals of flight time. Since the flight velocity increases with altitude, the spread of altitude between velocity measurements also increases with altitude in this case. However, if the data exist in continuous form, these wind data points could be obtained in whatever increment is desired.

The particular advantage of the α -vane technique of wind measurement is that an instantaneous and continuous record of winds experienced by a particular missile is available. It would seem that this wind-measuring scheme would be employed whenever direct measurements of launch vehicle loads are attempted. The main disadvantage of this technique is the accuracy and high-frequency response required of the instrumentation, particularly the angle-of-attack sensor. These requirements result in a very costly measurement scheme, usable for monitoring specific flights but not particularly attractive as a routine wind data collection system.

Smoke-Trail Method

The second technique of measuring detailed winds, the smoke-trail method, has been described in references 10 and 11. A schematic diagram of the measurement setup is shown in figure 4. It is an optical-photographic method of deducing wind velocities by triangulation from two cameras taking photographs of a visible trail of smoke left by an ascending rocket. The smoke may be the visible exhaust trail left by some rockets, or may be artificially generated by chemical releases into the airstream. The individual particles of smoke reach equilibrium with the atmosphere within seconds after the passage of the rocket. Two cameras, located about ten miles from the launch site, take synchronized pictures of the trail in known time increments. Triangulation is then used on a set of these photographs to determine the position of points along the smoke trail, usually in 100-foot-altitude increments though smaller increments are possible. Then, using position data from two sequential sets of pictures and the time interval between the pictures, the wind-velocity profile is found. All the data are obtained within about 2 minutes after the rocket is launched.

An example of the data obtained by the smoke-trail method from reference 10 is presented in figure 5. The winds measured on this particular day were low, less than 100 ft/sec, but a measurement of velocity was obtained for each 100-foot change in altitude. The short wavelength variations in wind velocity, or horizontal gusts, are very apparent.

For comparison, an averaged smoke-trail profile is presented in figure 5 also. This is smoke-trail data which have been averaged over

2,000-foot-altitude increments, the same altitude increment used in reducing balloon data. This profile is similar to the one which would have been measured by a balloon if it were capable of sensing the wind over the entire altitude range in the same time as the smoke trail. The short wavelength wind variations have been filtered out, although the gross wind motion remains.

This method of measuring detailed wind profiles has several advantages. First of all, since it uses precision photographic equipment, it is very accurate. (An estimate of rms error appears in ref. 8, and for a typical setup, is less than 1/2 ft/sec over the altitude range of interest.) Since horizontal wind velocities can be measured in altitude increments of less than 100 feet, gust wavelengths of importance to all vehicles in the foreseeable future can be obtained. The technique can be used to measure winds acting on a particular launch vehicle by equipping the vehicle with a small smoke generator. It is also suited for use with a relatively inexpensive sounding-rocket system for collecting routine wind data.

The principal disadvantage of the smoke-trail method is its current restriction to use on clear days with good visibility conditions. However, high jet stream winds are not dependent on visibility conditions near the ground so that the probability of measuring high winds on a clear day is just as good as on a cloudy day. In fact, profiles having peak wind speeds of 300 ft/sec have been measured by the method.

ANALYSIS

The response of a launch vehicle to some of the wind profiles just discussed has been determined using equations and a digital computer program developed by Mr. V. L. Alley of Langley Research Center. The equations are derived for small perturbations in the pitch plane about a zero-lift reference trajectory as indicated in figure 6. The degrees of freedom included in the equations are translation normal to the reference trajectory, pitching, and three elastic bending modes. The coefficients of these equations vary with time due to changing mass and aerodynamic properties. A closed-loop attitude and attitude-rate control system, including structural feedback and a stabilizing filter network, is also represented by the equations.

The wind responses to be shown are those of a Scout four-stage, solid-propellant vehicle. It has both thrust vector and aerodynamic control obtained by utilizing jet vanes and movable fin tips. The first bending frequency of the vehicle is about 3 cps. The Scout lifts off under about 3g acceleration and the maximum dynamic pressure is about 3,000 psf.

RESULTS OF WIND RESPONSE STUDIES

The Scout vehicle has been analytically flown through eight detailed wind profiles. Four profiles were obtained by the α -vane method and four by the smoke-trail method. The vehicle was also flown through a balloon-measured profile or a smoothed profile in each case.

 α -Vane Measured Profiles

Response time histories.- Typical time histories of vehicle response to the detailed, α -vane measured profile previously illustrated are shown in figure 7. On the upper curve the input wind velocity is shown as a function of time. This measured profile has been converted from an altitude to a time base using the reference trajectory for this particular launching. The wind input to the program is a series of points versus time, connected by straight lines between the points. For the portion of the flight illustrated, the winds never exceed about 70 ft/sec. The middle curve is the pitch angle perturbation of the complete vehicle. Lightly damped low-frequency oscillations of the rigid-body stability mode at about 1 cps are excited by the wind and are very apparent. The bottom curve is the rotation angle of the jet vanes and the aerodynamic fin tip controls. A control angle with the same sign as the pitch angle produces a restoring moment on the vehicle. The low-frequency stability mode frequency at 1 cps is also predominant in the control angle. However, oscillations at about 3 cps, corresponding to the first elastic bending mode, show that the detailed wind profile is exciting the structural modes of the vehicle and is being sensed by the control system via the mechanism of structural feedback.

The loads experienced by the vehicle are illustrated by the time histories in figure 8. The bending-moment response is shown for two wind profiles - at the bottom is the response to the same α -vane profile used in the previous figure, and at the top is the response to a radio-sonde balloon profile measured at approximately the same time. The bending moment shown here, and in subsequent figures, is at an inter-stage station on the vehicle near the location of maximum bending moment. It is recognized that the exact nature of the bending-moment response will vary with vehicle station, due to the influence of the various bending modes. However, only this one station will be examined in order to simplify the comparisons to be made. The oscillatory nature of the bending-moment response is very apparent. The detailed profile has caused a considerable increase in first-mode excitation, compared to the balloon profile, but it has also considerably increased the response of the low-damped stability mode near 1 cps. If an envelope of the maximum bending moments were drawn about these responses, as indicated on the

figure, the load levels due to the detailed profile would be generally higher than the load levels due to the balloon-measured profile.

Bending-moment envelope.- The bending-moment envelopes for the responses just illustrated are shown in figure 9. The bending moments have been normalized by the limit bending moment at the same station and are plotted over the altitude range from launch to about 50,000 feet. One curve is shown for the detailed α -vane measured profile, another for the radiosonde measured profile. For most altitudes, the detailed profile produces larger loads. The maximum moment induced on the structure by the radiosonde profile occurs in the 25,000- to 30,000-foot-altitude range and equals the detailed profile moments in this region. However, the α -vane profile produces greater loads at other altitudes. Its maximum occurs between 30,000- and 35,000-foot altitude and is about 15 percent greater than the maximum moment produced by the radiosonde profile. Most of this increase in bending moment comes from the excitation of the elastic modes by the detailed profile. However, at the lower altitudes, it has been shown that the detailed profile also excites the lightly damped pitching mode of this vehicle which increases the load. The bending moments which result from flying these profiles never exceed about 37 percent of limit load, reflecting the fact that these are relatively low winds with a peak velocity of about 115 ft/sec.

Effect of direction.- All of the wind profiles have been flown as headwinds. One profile, the α -vane measured wind used in the previous illustrations, was also flown as a tailwind and the result is shown in figure 10. The envelope of the ratio of bending moment to limit bending moment is shown for altitudes up to about 50,000 feet altitude for the profile flown both as a headwind and as a tailwind. The vehicle is flying a pitch program such that it is inclined about 35 degrees from the vertical in the maximum dynamic-pressure region near 35,000 feet altitude. Thus, headwinds induce slightly larger angles of attack than tailwinds. Headwinds are shown to produce the largest loads, in agreement with the larger wind angle of attack. Bending moments are actually about 5 percent lower in the maximum q region when the profile is flown as a tailwind. At lower altitudes, where the vehicle is flying nearly vertical, only very small differences are detectable.

Smoke-Trail Measured Profiles

Bending-moment responses similar to those just discussed for α -vane profiles are found for wind profiles determined by the smoke-trail method. A typical example of response to a smoke-trail profile (not the profile illustrated in fig. 5) is given in figure 11. The envelope of the ratio of bending moment to limit bending moment at the same station is given as a function of altitude. Envelopes are given for loads resulting

from both smoke-trail and averaged smoke-trail data. These data are for a case with a large wind shear in the maximum dynamic-pressure region with very little gustiness imposed on the shear. At lower altitudes, the smoke-trail data show considerable short wavelength variation in wind velocity. This is reflected in the bending-moment envelopes by the increase in detailed profile loads, compared to the smoothed profile loads, at lower altitudes and only a slight increase, about 5 percent, in the peak wind region. Notice that the maximum bending moment is only about 30 percent of the limit load. Again, this results from the low peak wind velocities of about 115 ft/sec.

Bending-Moment Amplification by Detailed Profiles

The bending-moment envelopes just discussed have shown that the detailed profiles generally produce higher loads than the balloon-type profiles. The actual amplification of the bending moment at various altitudes is illustrated in figure 12 for three wind measurements. The bending-moment envelope of the detailed profile has been divided by the envelope of bending moment for the smoothed profile, such that, at any altitude, the ordinate gives the increase in load produced by the detailed profile. All three profiles had peak wind velocities of about 115 ft/sec such that maximum steady wind loads would be comparable. The amplification by the detailed profiles at various altitudes is seen to vary drastically with the particular case, illustrating the dependence of the load on the details of the profile. Not only does the amplification of the load depend on the details of the particular profile, but it also depends on the characteristics of the particular vehicle being considered. (In addition, this factor will reflect any changes in wind velocity which occur between the time of the detailed and the balloon measurements.) The large amplifications shown here do not necessarily endanger this vehicle, since it has been designed for a much higher peak wind with an added margin for gusts. Also, some of the largest amplifications occur in the low- or high-altitude regions, where dynamic pressure is reduced, so that total loads are within design limits.

The increase in bending moments which results from using the detailed profiles instead of the smoothed or averaged profiles can be generally credited to the short wavelength fluctuations, or "gustiness," of the detailed profiles. However, high gross winds and large gusts do not necessarily occur at the same time. Thus, it can be argued that, since most of the detailed wind profiles have been measured on relatively low wind days, the amplification of bending moment by the detailed fluctuations of these profiles may exaggerate the effect to be expected on high wind days. Figure 13 is an attempt to establish the trend of the bending-moment amplification as the peak wind velocity increases. The ratio of the maximum bending moment resulting from the detailed profiles to the maximum bending moment resulting from the smoothed profiles is

plotted against the peak wind velocity of the detailed profile. The bending moments presented are those which occur in the maximum dynamic-pressure portion of the launch trajectory. The circles indicate profiles obtained by the smoke-trail method and the squares indicate profiles measured by the α -vane method. Considerable scatter is evident in these points, but a trend does appear to be indicated. Larger amplifications occur at low peak wind velocities, while continually decreasing amplifications occur as the peak wind velocity increases. The scatter evident here is partially due to the difficulty of obtaining radiosonde balloon data at the same time as the detailed profile measurement. From 30 minutes to 5 hours time difference exists in these soundings, providing time for the wind profile to have changed. Of course, much of the scatter is simply due to the dependence of the bending-moment response on the details of the particular profile and the particular vehicle. For instance, the α -vane profile which produces amplifications greater than two for a peak wind velocity of 117 ft/sec was a particularly "gusty" profile. However, this figure does seem to indicate that detailed wind profiles with very high peak winds will amplify the bending moments produced by the smoothed profiles by only moderate amounts.

Much additional data are needed. The variations in bending moment which result from response to the various profiles indicate the importance of the characteristics of the particular profile. Though considerably more experience with these profiles, as applied to various vehicles, is needed, a possible design approach would be similar to the one recommended in reference 5. It would be a brute force method by which samples of measured, detailed wind profiles (possibly 15, 50, or 150 profiles) would be used to predict loads on a launch vehicle. Such a technique would require a massive computer program involving variable parameters and elastic degrees of freedom, but it would not necessitate separate consideration of winds and gusts. A more sophisticated approach would be the use of a statistical method such as proposed in references 12 and 13.

CONCLUDING REMARKS

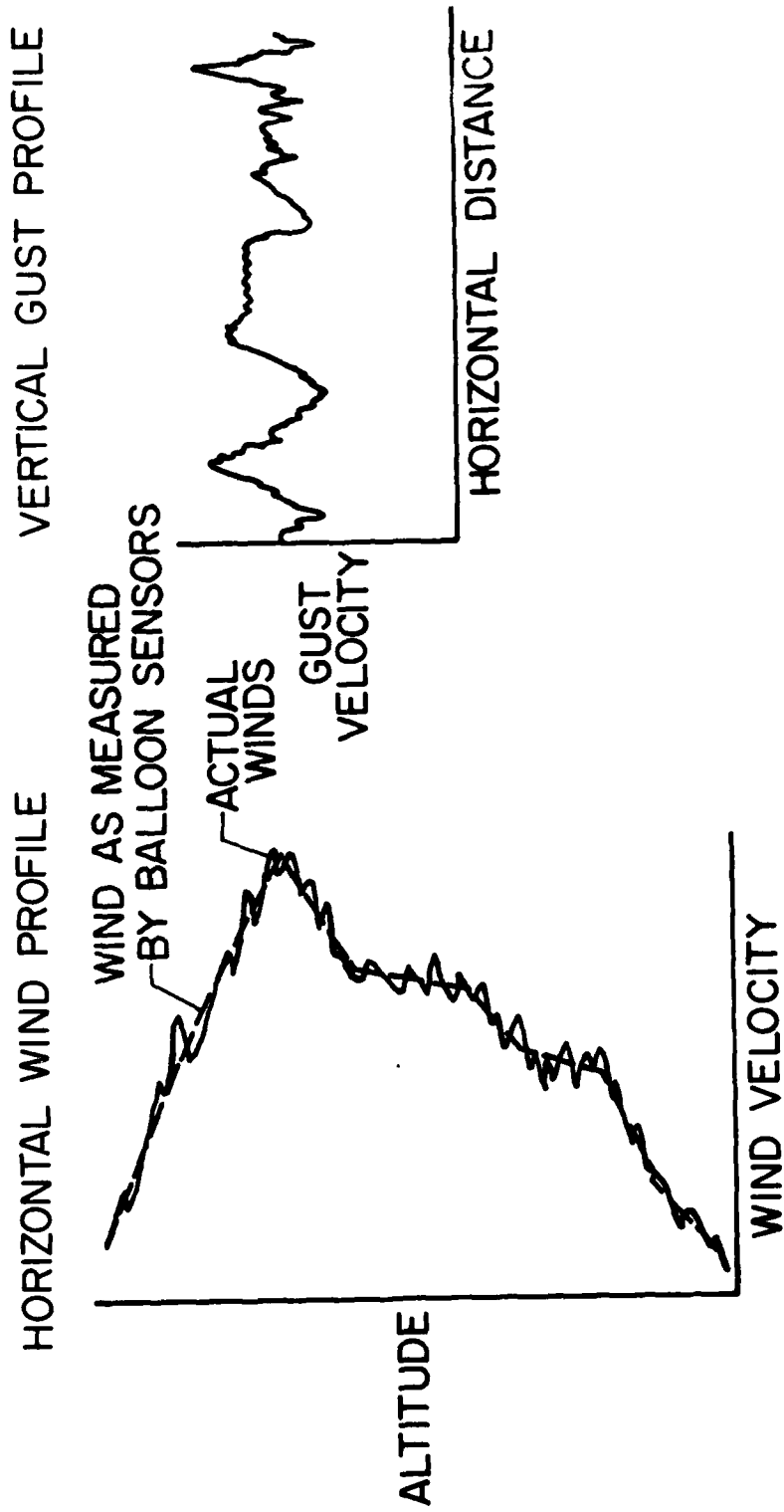
Detailed wind profiles obtained by two methods have been discussed. The two methods of measuring horizontal wind velocity as a function of altitude, the α -vane method and the smoke-trail method, utilize an angle-of-attack measuring device carried by a launch vehicle and a trail of smoke left by a sounding rocket, respectively, to sense the motion of the atmosphere. A launch vehicle has been analytically flown through a number of these detailed profiles as well as equivalent balloon-measured or smoothed profiles. The detailed wind profiles were shown to excite the pitch and elastic bending modes of the vehicle and, as

a result, to produce higher loads on the vehicle structure than are produced by balloon-type wind profiles. Present design procedures (which are based on balloon-measured profiles) allow for this increased load by adding a somewhat arbitrary gust load to the wind load. When more of the detailed wind profile data are available, revision of design procedures to include the detailed variations in the winds would seem to be indicated.

REFERENCES

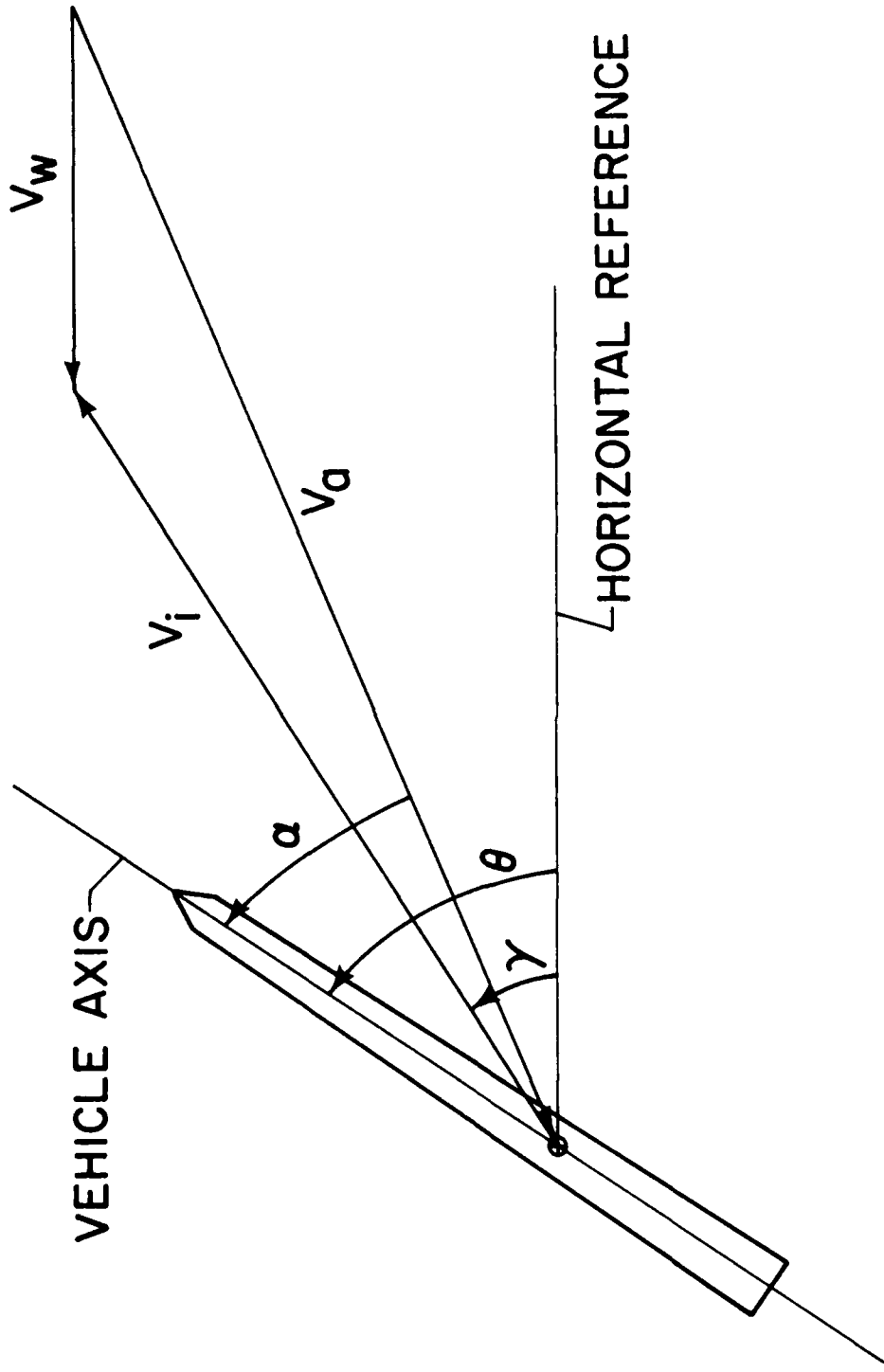
1. Sissenwine, Norman: Windspeed Profile, Windshear, and Gusts for Design of Guidance Systems for Vertical Rising Air Vehicles. Air Force Surveys in Geophysics No. 57 (AFCRC-TN-54-22), Air Force Cambridge Research Center, November 1954.
2. Sissenwine, Norman: Development of Missile Design Wind Profiles for Patrick AFB. Air Force Surveys in Geophysics No. 96 (AFCRC-TN-58-216, ASTIA Document No. AD-146 870), Air Force Cambridge Research Center, March 1958.
3. Mazzola, Luciano L., Hobbs, Norman P., Frassinelli, Guido J., and Criscione, Emanuel S.: Development of Interim Wind, Wind Shear, and Gust Design Criteria for Vertically-Rising Vehicles. WADD TR 59-504, 1959.
4. Scoggins, James R., and Vaughan, William W.: Description of Wind Shears Relative to a Missile/Space-Vehicle Axis and a Presentation of the Cape Canaveral, Florida, 95 and 99 Percent Probability Level Standardized Wind Profile Envelopes (1-80 KM) and Associated Wind Shears for Use in Design and Performance Studies. MTP-AERO-61-48, June 8, 1961.
5. Mazzola, Luciano L., Hobbs, Norman P., and Criscione, Emanuel S.: Wind, Wind Shear, and Gust Design Criteria for Vertically-Rising Vehicles as Recommended on the Basis of Montgomery, Alabama, Wind Data. WADD TR 61-99, 1961.
6. Donely, Philip: Summary of Information Relating to Gust Loads on Airplanes. NACA TR 997, 1950.
7. Pratt, Kermit G., and Walker, Walter G.: A Revised Gust-Load Formula and a Re-Evaluation of V-G Data Taken on Civil Transport Airplanes From 1933 to 1950. NACA TR 1206, 1954.
8. Press, Harry, and Steiner, Roy: An Approach to the Problem of Estimating Severe and Repeated Gust Loads for Missile Operations. NACA TN 4332, 1958.
9. Reisig, Gerhard H. R.: Instantaneous and Continuous Wind Measurements Up to the Higher Stratosphere. Jour. of Meteorology, vol. 13, no. 5, October 1956, pp. 448-455.
10. Tolefson, Harold B., and Henry, Robert M.: A Method of Obtaining Detailed Wind Shear Measurements for Application to Dynamic Response Problems of Missile Systems. Jour. of Geophysical Research, vol. 66, no. 9, September 1961, pp. 2849-2862.

11. Henry, Robert M., Brandon, George W., Tolefson, Harold B., and Lanford, Wade E.: The Smoke-Trail Method for Obtaining Detailed Measurements of the Vertical Wind Profile for Application to Missile-Dynamic-Response Problems. NASA TN D-976, 1961.
12. Trembath, N. W.: Control System Design Wind Criteria. STL GM-TM-0165-00258, June 30, 1958.
13. Bieber, R. E.: Missile Structural Loads by Nonstationary Statistical Methods. IAS Journal, vol. 28, no. 4, April 1961, pp. 284-294.



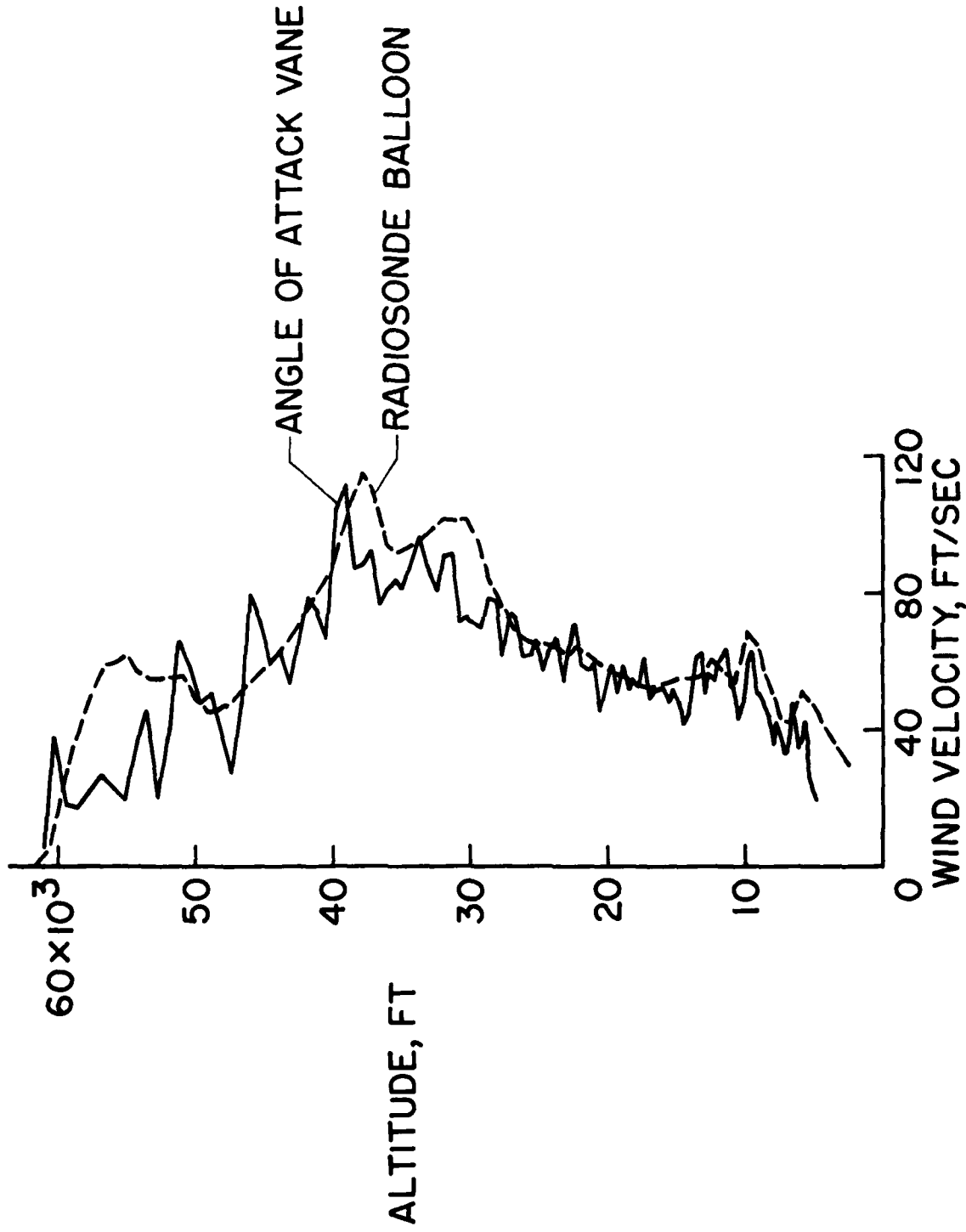
NASA

Figure 1.- Types of available wind and gust data.



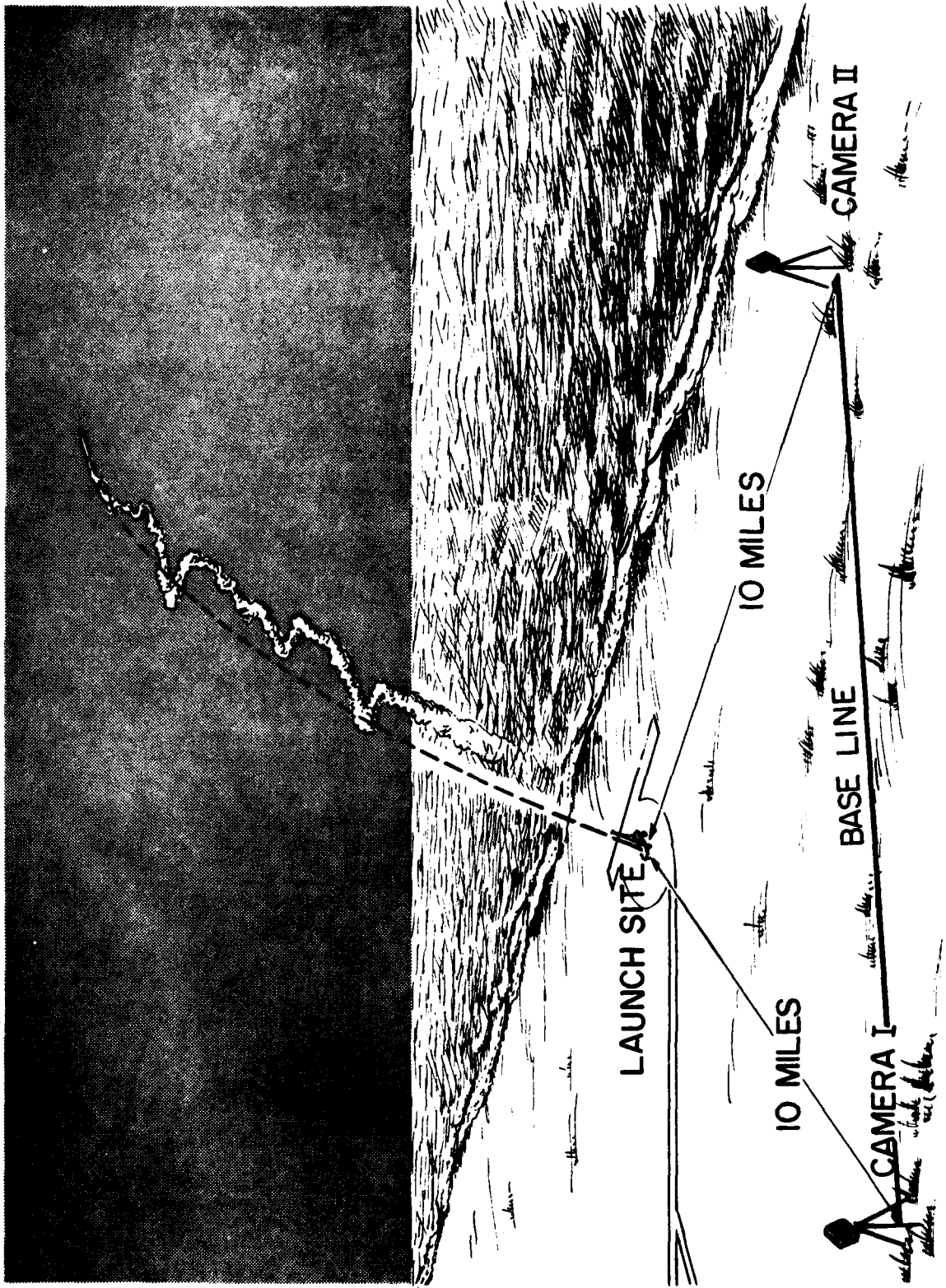
NASA

Figure 2.- Wind measurement using an angle-of-attack sensor.



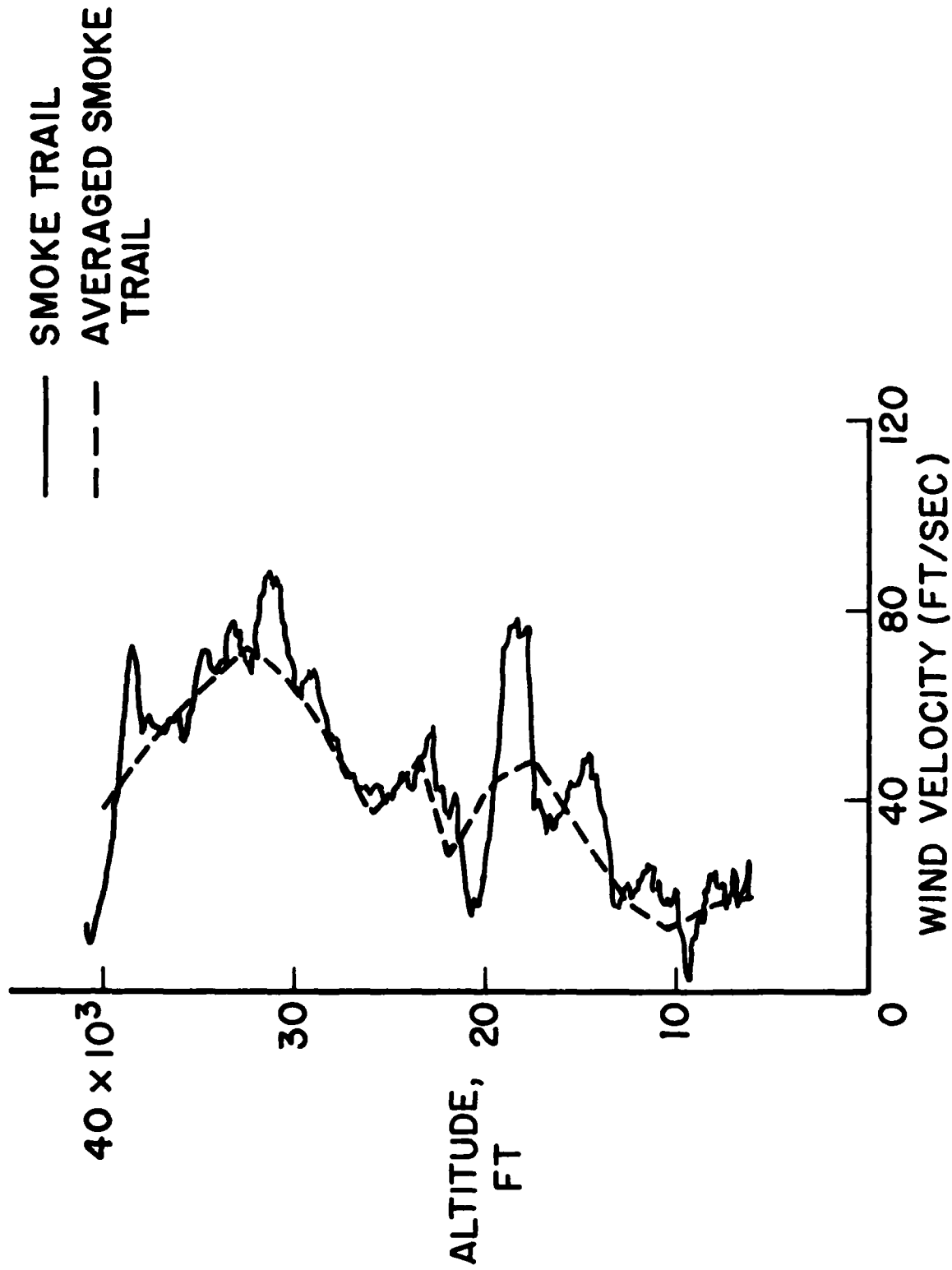
NASA

Figure 3.- Wind profiles measured using angle-of-attack sensors and radiosonde balloons.



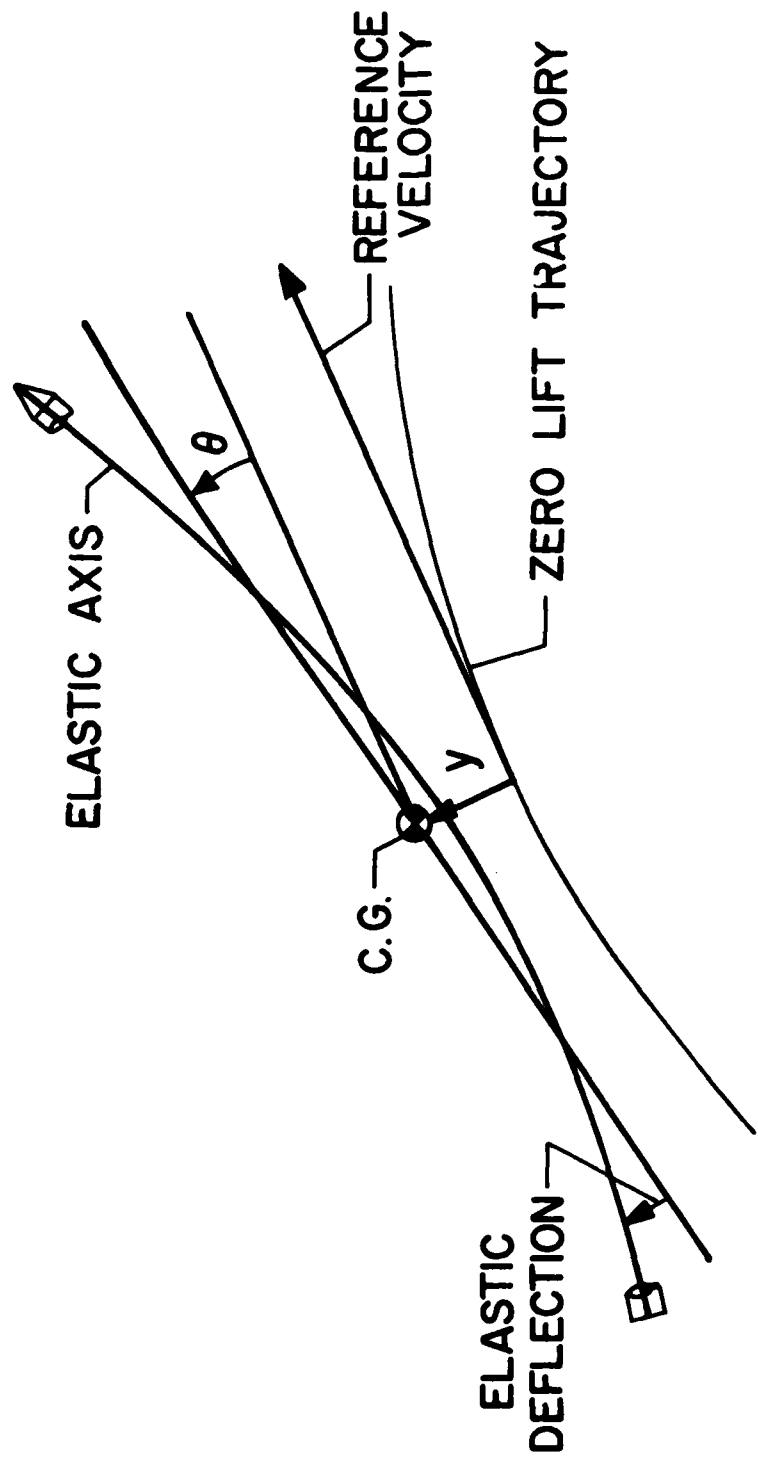
NASA

Figure 4.- Wind measurement by the smoke-trail method.



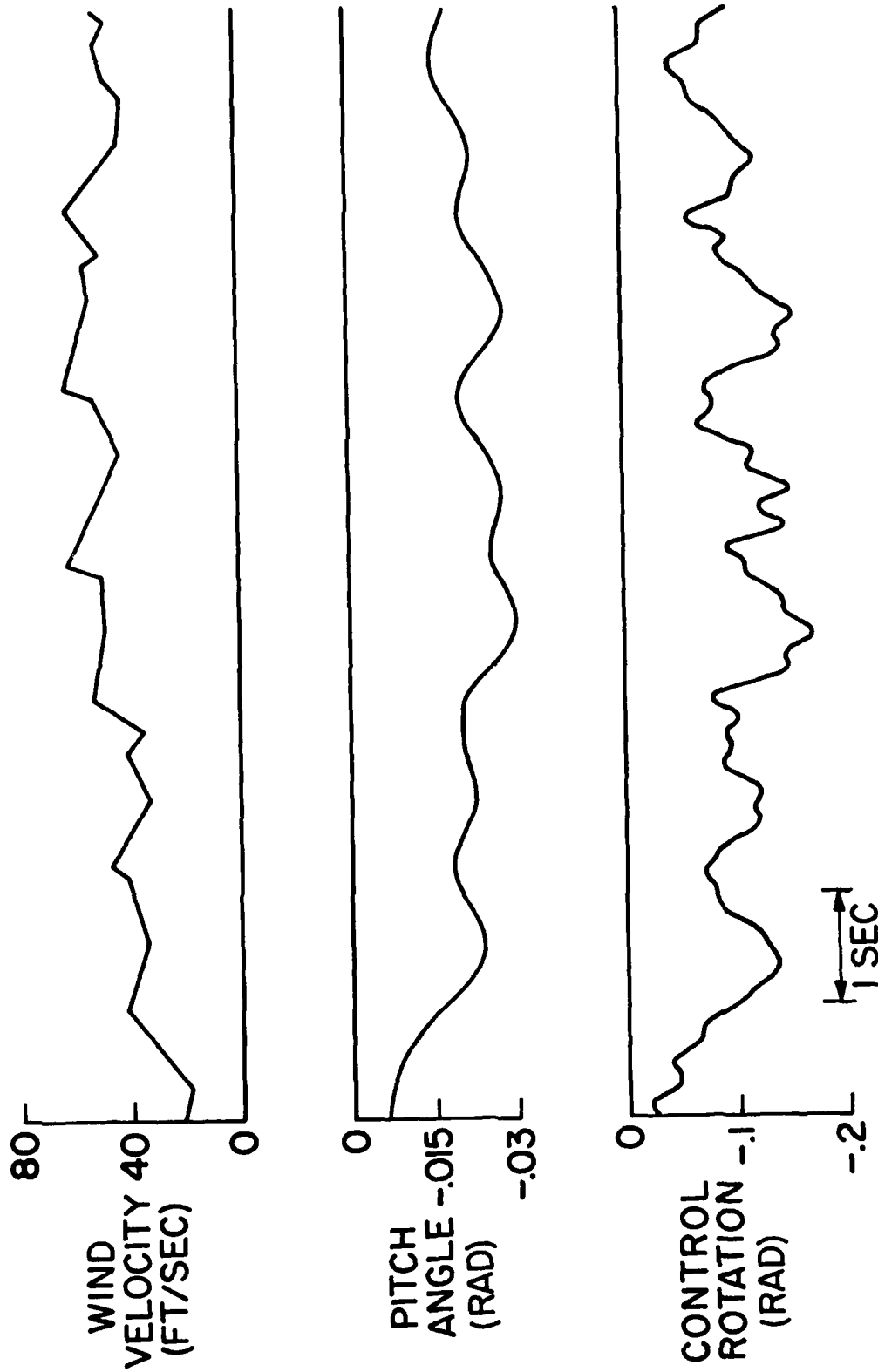
NASA

Figure 5.- Wind profiles measured by the smoke-trail method.



NASA

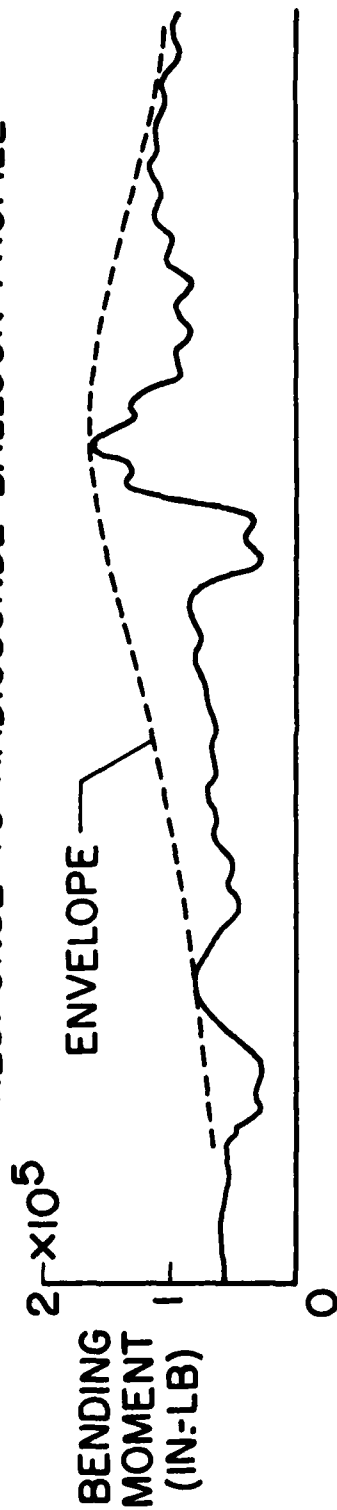
Figure 6.- Coordinate system used in the calculations.



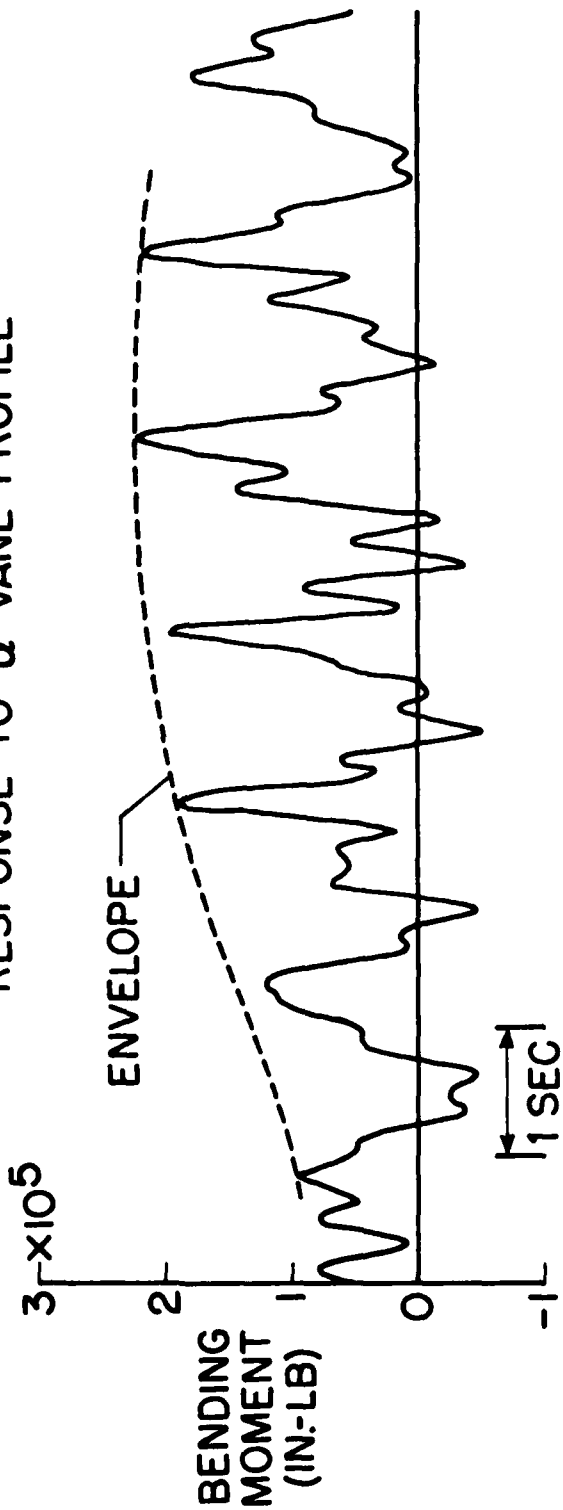
NASA

Figure 7.- Typical time histories of pitch angle and control rotation angle for flight through an α -vane measured wind profile.

RESPONSE TO RADIOSONDE BALLOON PROFILE

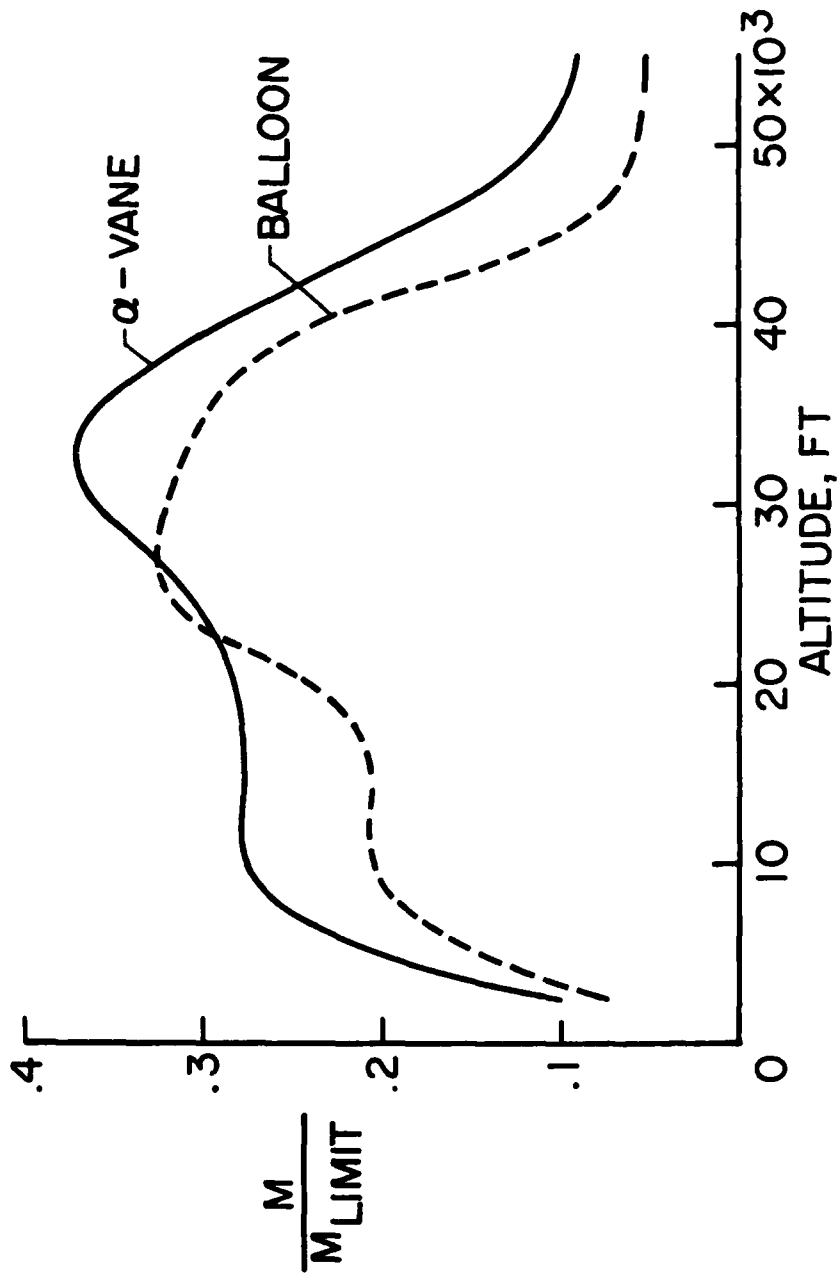


RESPONSE TO α -VANE PROFILE



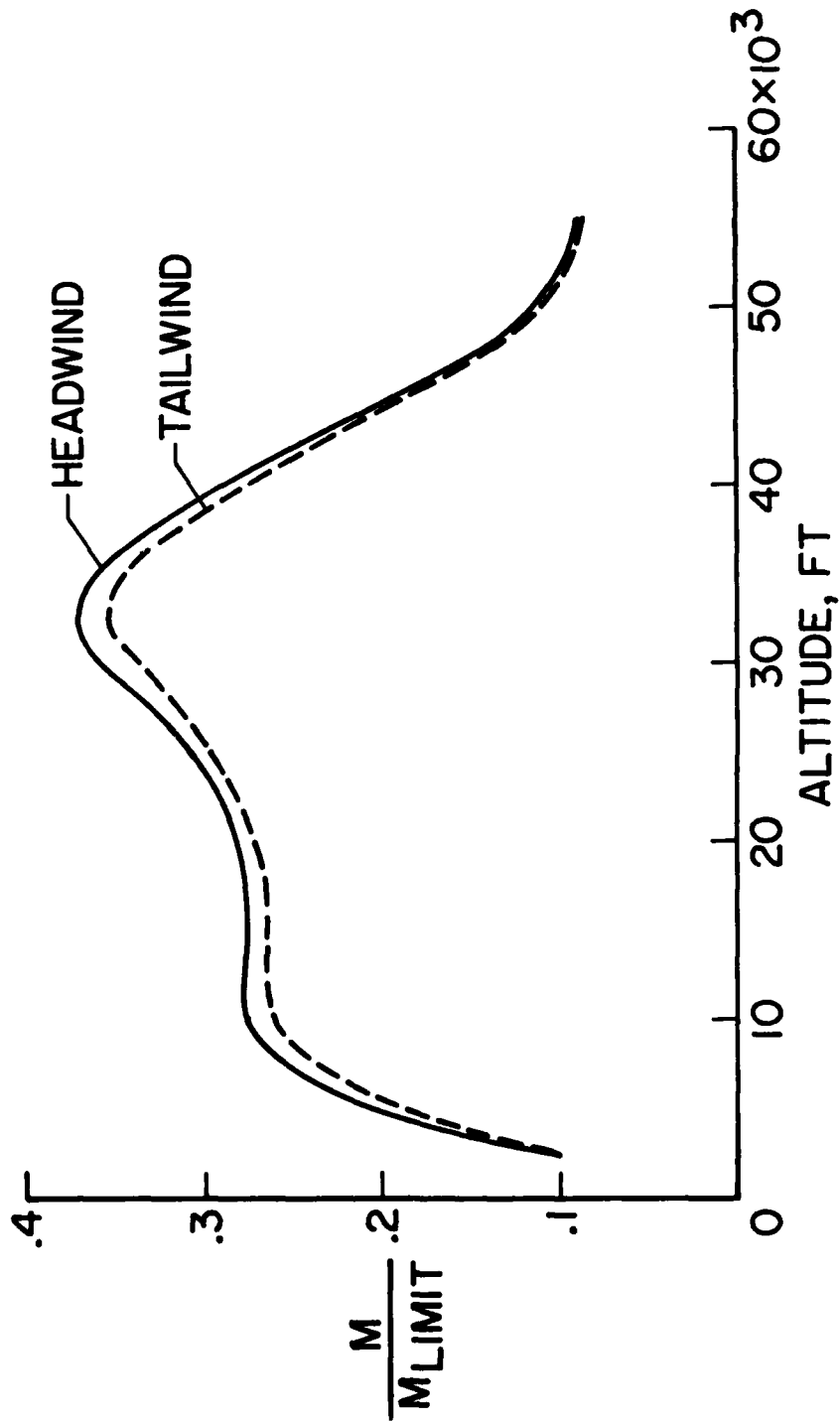
NASA

Figure 8.- Typical bending-moment time histories for flight through an α -vane measured profile and the equivalent radiosonde measured profile.



NASA

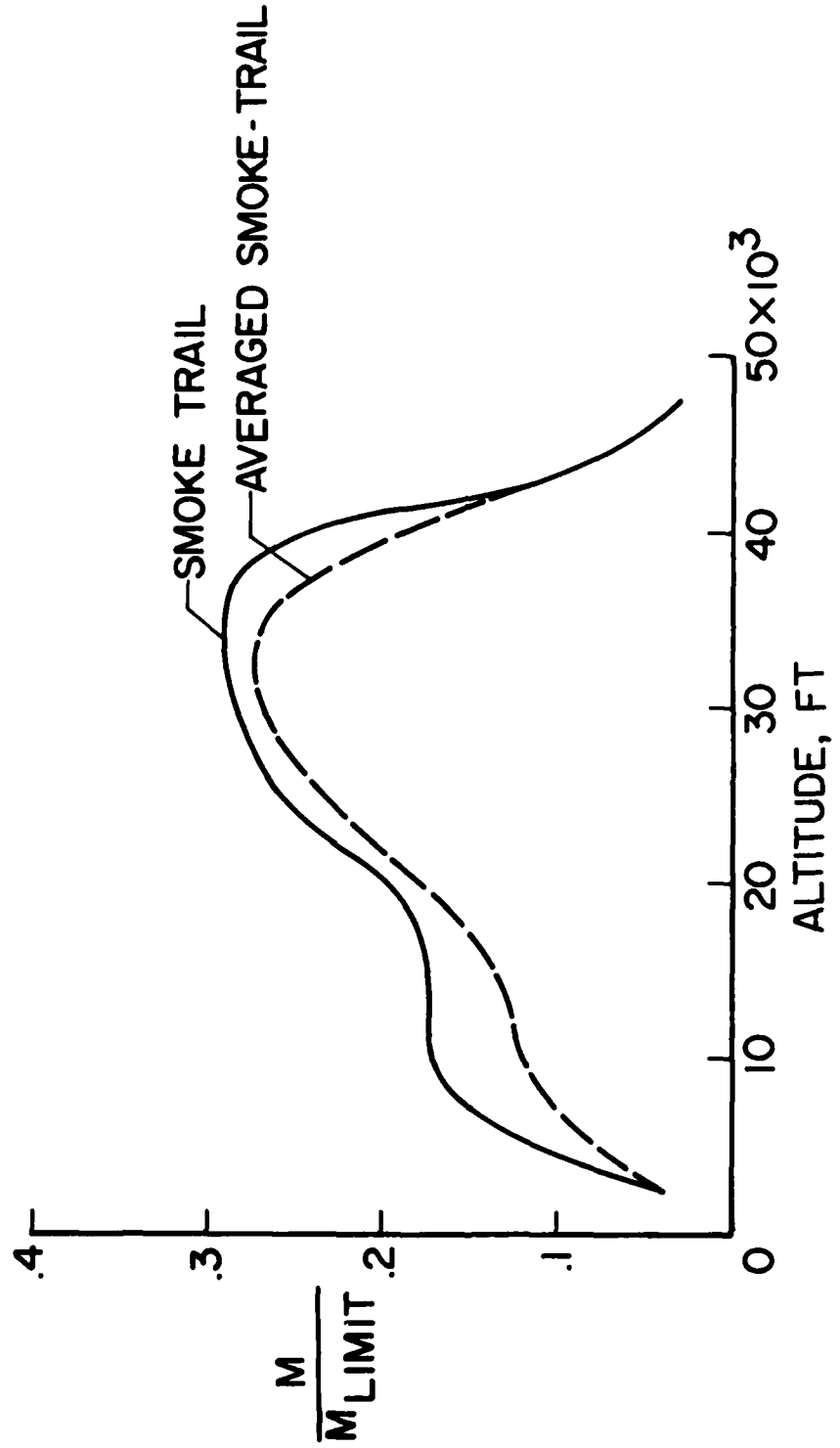
Figure 9.- Bending-moment envelopes for an α -vane measured profile and its equivalent balloon measured profile. Maximum $V_W = 115$ ft/sec.



NASA

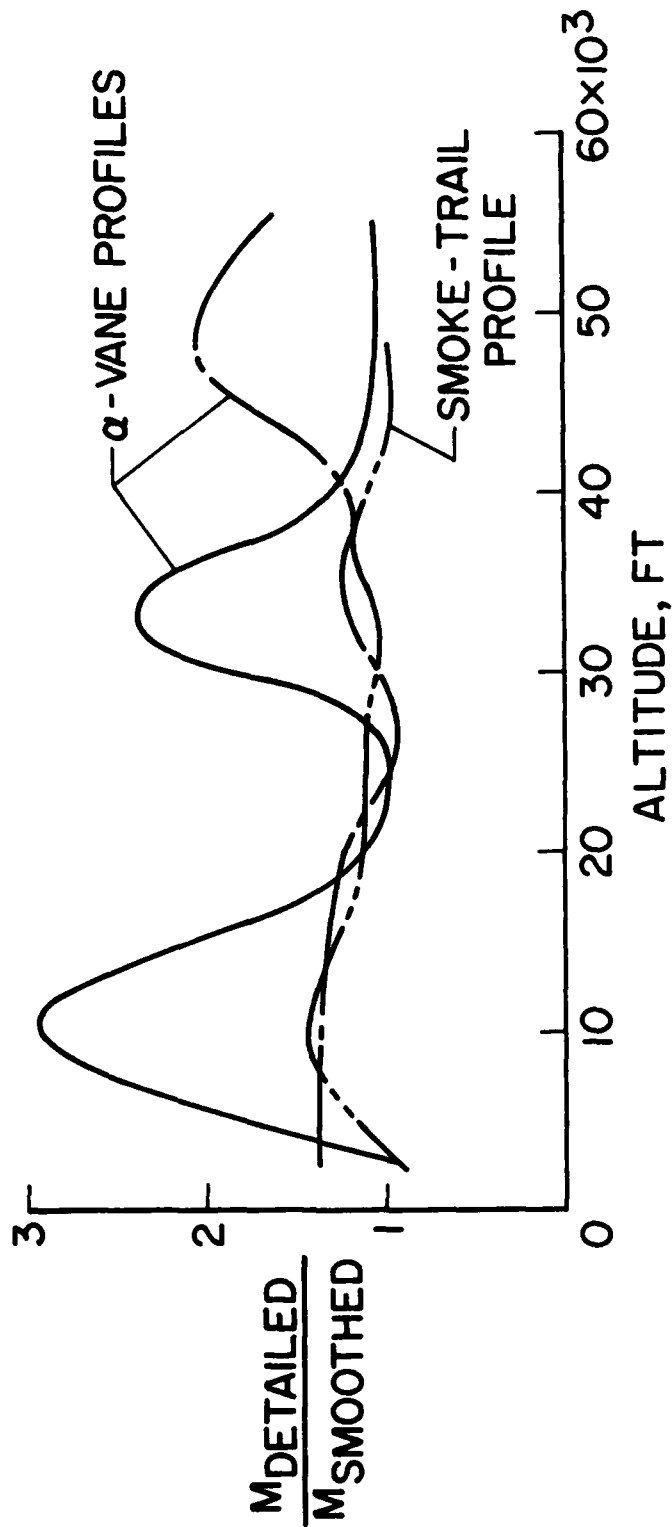
Figure 10.- Bending-moment envelopes for an α -vane measured profile flown as a headwind and a tailwind. Maximum $V_w = 115$ ft/sec.

SMOKE TRAIL PROFILES



NASA

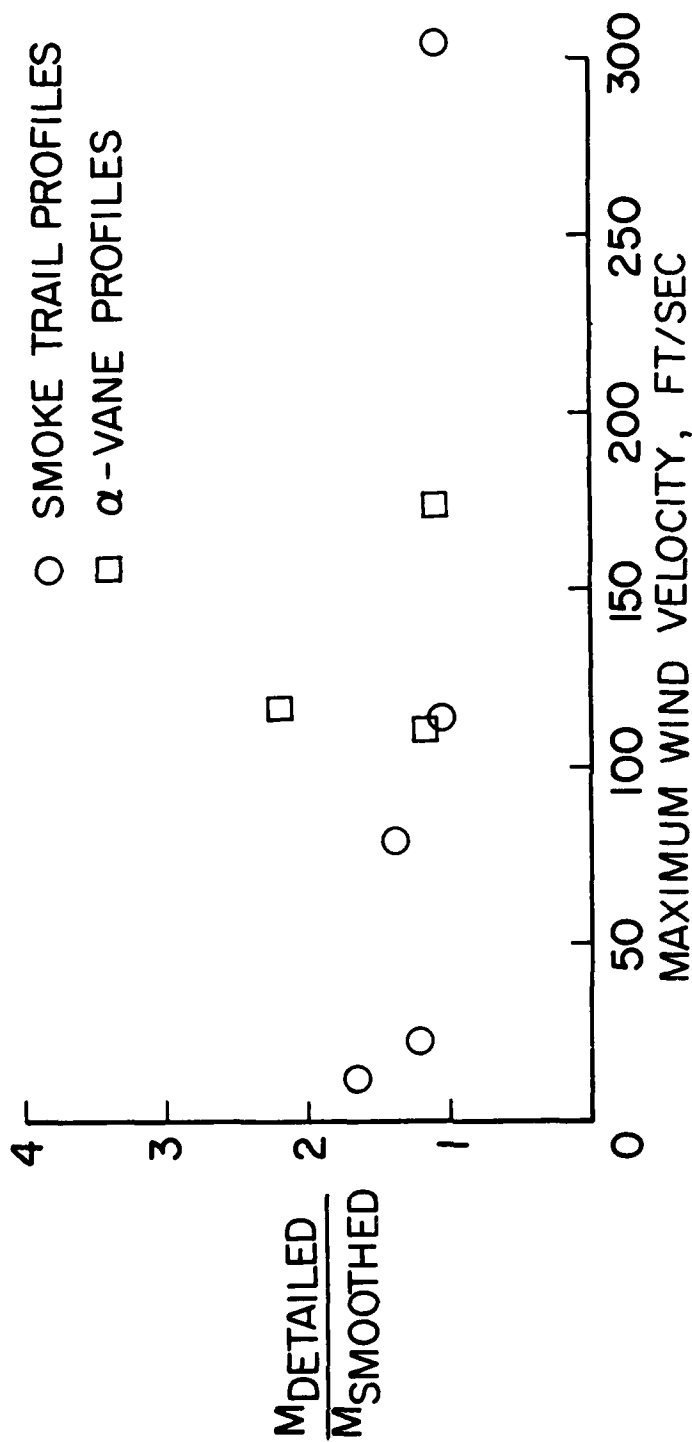
Figure 11.- Bending-moment envelopes for a smoke-trail profile and its averaged profile. Maximum $V_w = 114$ ft/sec.



NASA

Figure 12.- Bending-moment amplification as a function of altitude for three wind soundings having maximum V_w of about 115 ft/sec.

LOAD AMPLIFICATION AT MAX. Q



NASA

Figure 13. - Bending-moment amplification by detailed wind profiles near maximum dynamic pressure.